Chapter 5

Satellite Ocean-Color Validation Using Ships of Opportunity

Robert Frouin, David L. Cutchin, Lydwine Gross-Colzy and Antoine Poteau

Scripps Institution of Oceanography, University of California San Diego, La Jolla

Pierre-Yves Deschamps

Laboratoire d'Optique Atmosphérique, Université des Sciences et Technologie de Lille, France

5.1 INTRODUCTION

The investigation's main objective is to collect from platforms of opportunity (merchant ships, research vessels) concomitant normalized water-leaving radiance and aerosol optical thickness data over the world's oceans. A global, long-term data set of these variables is needed to verify whether satellite retrievals of normalized water-leaving radiance are within acceptable error limits and, eventually, to adjust atmospheric correction schemes.

To achieve this objective, volunteer officers, technicians, and scientists onboard the selected ships collect data from portable SIMBAD and Advanced SIMBAD (SIMBADA) radiometers. These instruments are specifically designed for evaluation of satellite-derived ocean color. They measure radiance in spectral bands typical of ocean-color sensors. The SIMBAD version measures in 5 spectral bands centered at 443, 490, 560, 670, and 870 nm, and the Advanced SIMBAD version in 11 spectral bands centered at 350, 380, 412, 443, 490, 510, 565, 620, 670, 750, and 870 nm. Aerosol optical thickness is obtained by viewing the sun disk like a classic sun photometer. Normalized water-leaving radiance, or marine reflectance, is obtained by viewing the ocean surface through a vertical polarizer in a specific geometry (nadir angle of 45^o and relative azimuth angle of 135^o) to minimize direct sun glint and reflected sky radiation. The SIMBAD and SIMBADA data, after proper quality control and processing, are delivered to the SIMBIOS project office for inclusion in the SeaBASS archive. They complement data collected in a similar way by the Laboratoire d'Optique Atmosphérique of the University of Lille, France.

The SIMBAD and SIMBADA data are used to check the radiometric calibration of satellite ocean-color sensors after launch and to evaluate derived ocean-color variables (i.e., normalized water-leaving radiance, aerosol optical thickness, and aerosol type). Analysis of the SIMBAD and SIMBADA data provides information on the accuracy of satellite retrievals of normalized water-leaving radiance, an understanding of the discrepancies between satellite and in situ data, and algorithms that reduce the discrepancies, contributing to more accurate and consistent global ocean color data sets.

5.2 RESEARCH ACTIVITIES

Since November 2002, SIMBAD measurements were made during 7 research cruises of opportunity, bringing to 69 the number of campaigns with SIMBAD measurements realized during the period October 1996-Otober 2003. These 7 cruises, as well as ongoing and planned cruises, are listed in Table 1 with name of cruise, SIMBAD and SIMBADA instrument(s) used, region of measurements, name of operator, and dates of measurements. The data were collected In the Pacific Ocean, off the West Coast of the United States and Baja California, Mexico (CalCOFI and IMECOCAL cruises), between Peru and New Zealand (P500304), and between Australia and Papeete (BEAGLE2003, Leg1). The location of the measurements from the first 5 cruises, which have been processed, is displayed in Figure 5.1. The processed data (a total of 606 complete data sets) have been transferred to the SeaBASS archive.

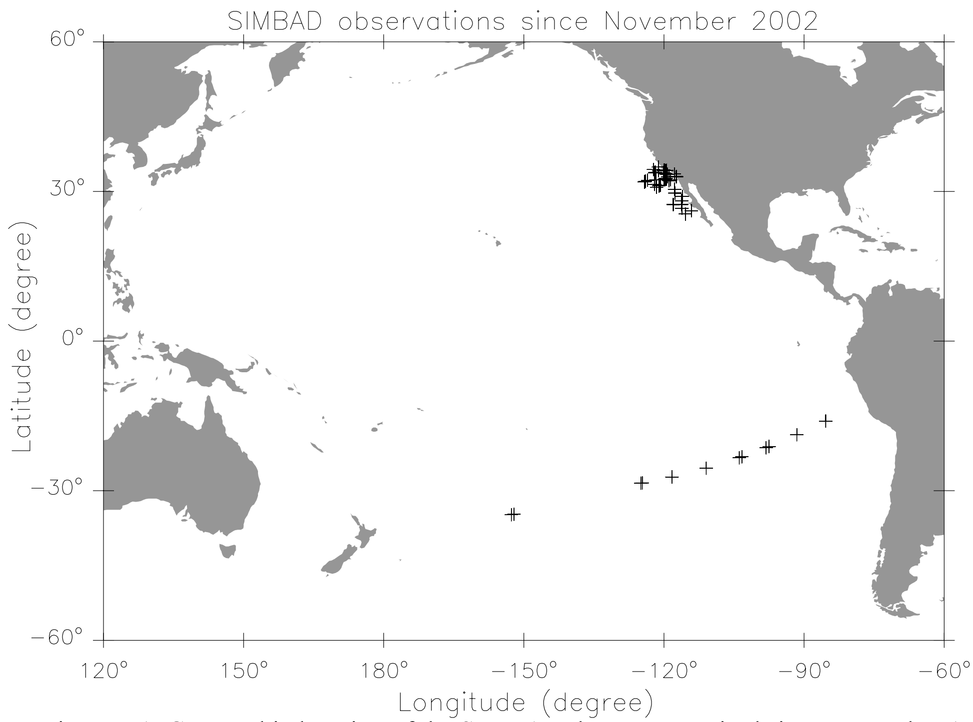

Figure 5.1: Geographic location of the SIMBAD data sets acquired since November 1, 2002.

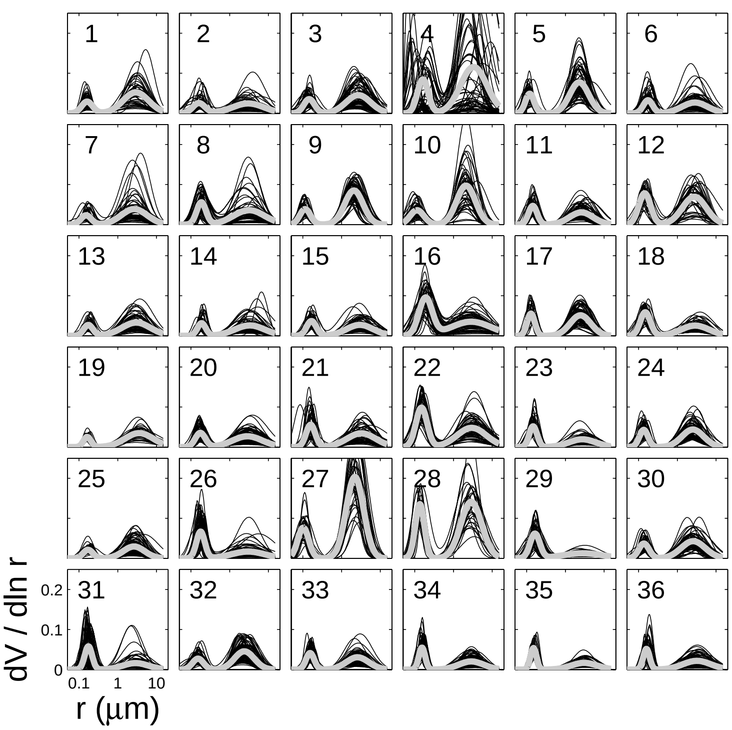

Figure 5.2: The calibrated 36 PRSOM neurons: Volume size distribution dV/dLnr. In each plot, the data gathered by the corresponding neuron is plotted in black, while their referent vector is plotted in gray.

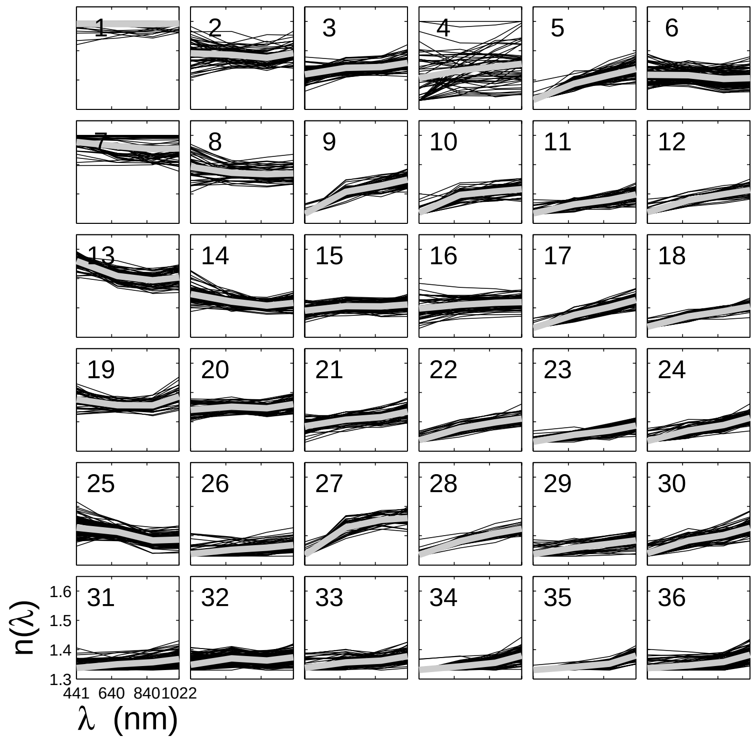

Figure 5.3: Same as Figure 5.2, but real part n of the refractive index

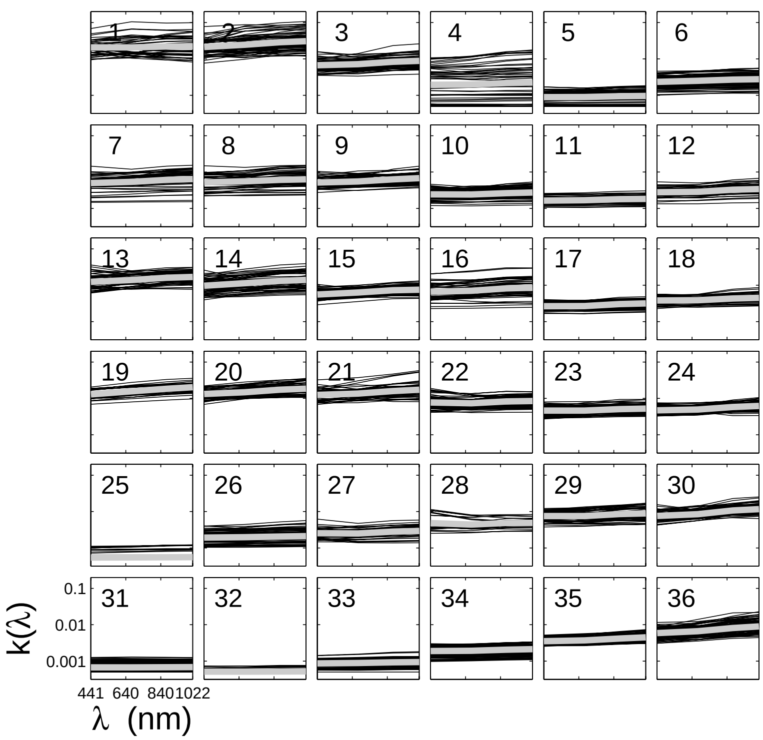

Figure 5.4: Same as Figure 5.2, but imaginary part k of the refractive index, plotted on a logarithmic scale.

Table 5.1. SIMBAD cruises during November 2002 –October 2003.

—IMECOCAL 0210/11,Ensenada-San Carlos, B/O Francisco de Ulloa, Simbad08, Jushiro Cepeda, 16 Oct - 06 Nov 02

—IMECOCAL 0301/02, Baja California, B/O Francisco de Ulloa, Simbad08, Jushiro Cepeda, 08 Feb - 15 Feb 03

—CalCOFI0304, Southern California Bight, R/V Roger Revelle , Simbad03, Haili Wang, 03 Apr - 27 Apr 03

—IMECOCAL 0304/05, Baja California, B/O Francisco de Ulloa, Simbad06, Jushiro Cepeda, 08 Apr - 22 Apr 03

—P500304, Southern Pacific, M/V Nacre, Simbad 07 David Cutchin, 24 Apr - 5 May 03

—IMECOCAL 0307, Baja California, B/O Francisco de Ulloa, Simbad08, Martin de la Cruz, 01 Jul - 22 Jul 03

—BEAGLE2003, Leg1, Western Pacific, R/V Mirai, Simbad 03/07, SimbadA01, Brian Irvin, 03 Aug - 06 Sep 03

—BEAGLE2003, Leg2, Eastern Pacific, R/V Mirai, Simbad 03/07, SimbadA01, Gadiel Alarcon, 09 Sep - 16 Oct 03

—IMECOCAL 0310, Baja California, B/O Francisco de Ulloa, Simbad08, Martin de la Cruz, 10 Oct - 31 Oct 03

—BEAGLE2003, Leg3, Valparaiso-Santos, R/V Mirai, Simbad 03/07, SimbadA01, Vivian Lutz, 19 Oct - 02 Nov 03

—OAS1003, Western South Atlantic, R/V Aldebaran, Simbad06, SimbadA02, Denise Vizziano, 26 Oct – 04 Nov 03

The history of SIMBAD calibration coefficients and the accuracy of the view angles measured by the radiometers have been analyzed. This effort started during the first year of the investigation, but was continued the second and third years with additional data. Trends in the calibration coefficients and biases in the view angles were removed, and all the SIMBAD data acquired since October 1996 have been re-processed or processed with adjusted calibration coefficients. Several aspects of satellite ocean-color remote sensing have been examined. They include the selection of aerosol models for atmospheric correction, the SeaWiFS performance in varied oceanic regions, a new algorithm to retrieve marine reflectance and chlorophyll-a concentration based on principal component analysis of atmospheric effects, and the SeaWiFS radiometric calibration in the near infrared. An inversion scheme was also developed to retrieve aerosol scale height from POLDER and MERIS data. The main results and findings are summarized in the next section (see also, below, the list of publications since 2002).

5.3. RESEARCH RESULTS

Aerosol mixtures for ocean color remote sensing

A Probabilistic Self-Organizing Map (PRSOM) has been applied to AERONET retrievals of aerosol size distribution and refractive index at island and coastal sites (Figures 5.2, 5.3, and 5.4). The PRSOM suggests that there are two strong (likely) situations: weakly absorbing mixtures on the one hand, and absorbing dust or urban soot aerosols on the other hand. Intermediate situations are possible, but not probable. The weakly absorbing mixtures (Figure 5.5) are very different from the classical (Shettle and Fenn, 1979) aerosol models (Figures 5.6 and 5.7). If we assume that AERONET provides representative conditions for ocean color remote sensing, two important results have to be emphasized. First, the classical models allow one to process low values of the Angström exponent α (670), but these conditions may not be the most encountered, even in the open ocean. Second, the PRSOM mixtures indicate a different association between Angström exponent and single scatttering albedo. As expected, it is not possible to separate absorbing from weakly absorbing mixtures from a given (observed) ε (χ, 670, 865) (Figures 5.8 and 5.9). However, within one of the two types of situations, the PRSOM neurons can be clearly identified using a directional sampling of the ε parameter (case of POLDER & MISR). Figure 5.9 summarizes the directional behavior of ε using a principal component analysis. Three principal components restore 99% of the information The principal components of the weakly absorbing mixtures have the same range of variability as those of the absorbing mixtures (Figure 5.9b).

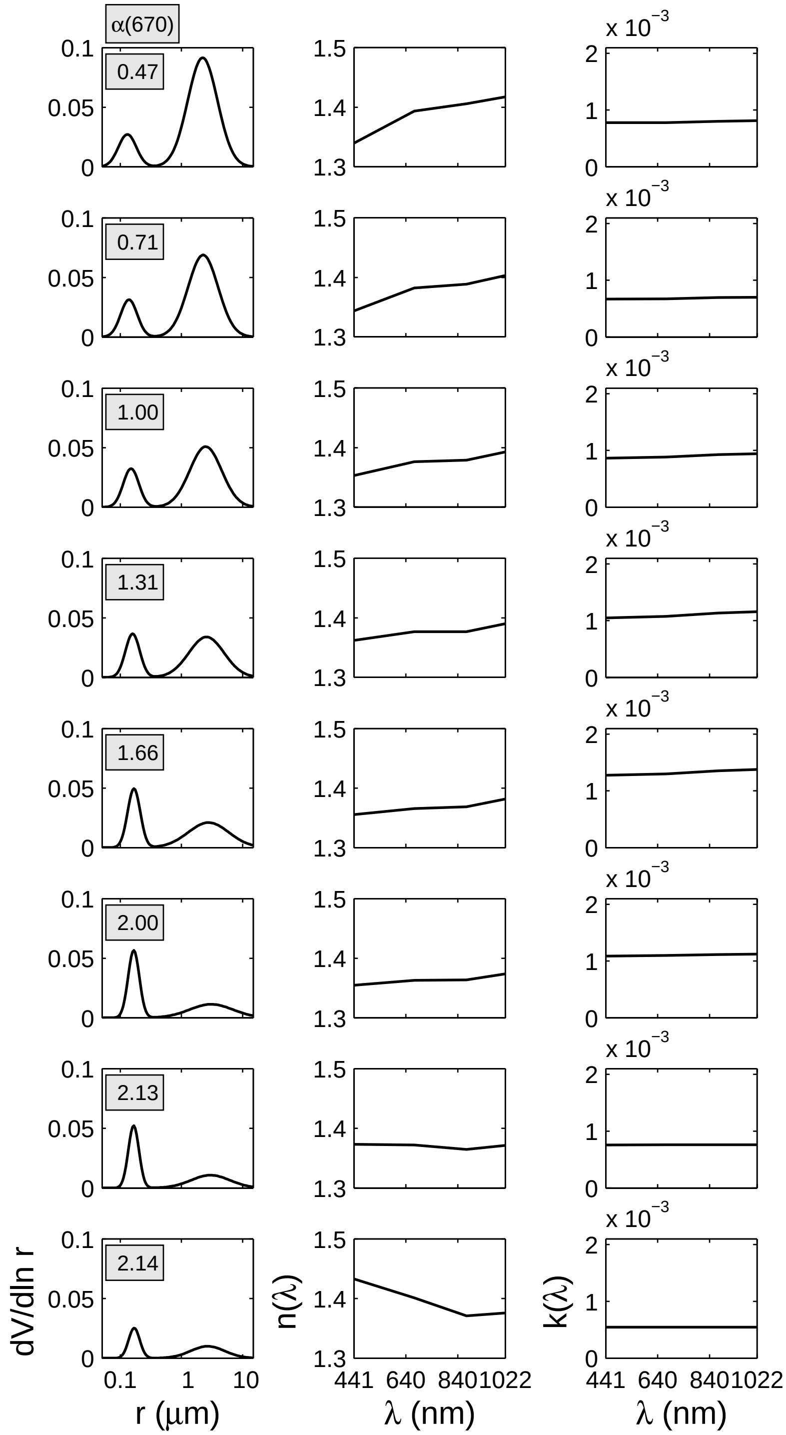

Figure 5.5: Gravity centers of the eight bins dividing the "open ocean" ensemble. First column is dV/dLnr, second column is n, and third column is k. In each plot of dV/dLnr, the corresponding Angström exponent, α(670) is indicated in a framed box.

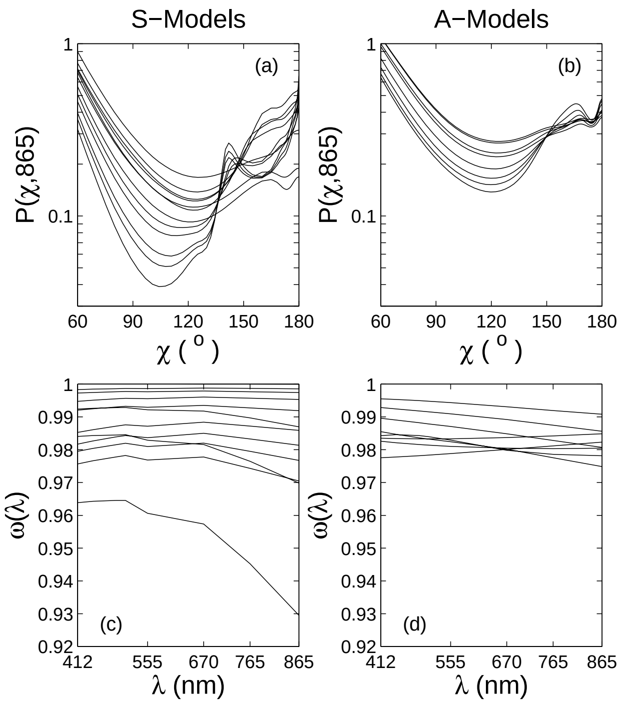

Figure 5.6: Phase function and single scattering albedo of the Standard (S-) models, (a) and (c), and of the AERONET (A-) models, (b) and (d).

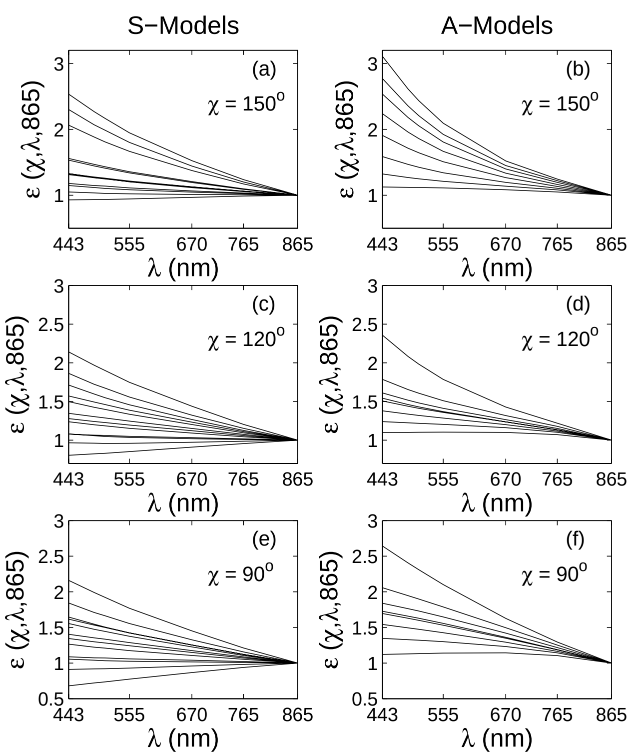

Figure 5.7: Spectral behavior of ε for the two sets of aerosol models and three scattering angles, χ.

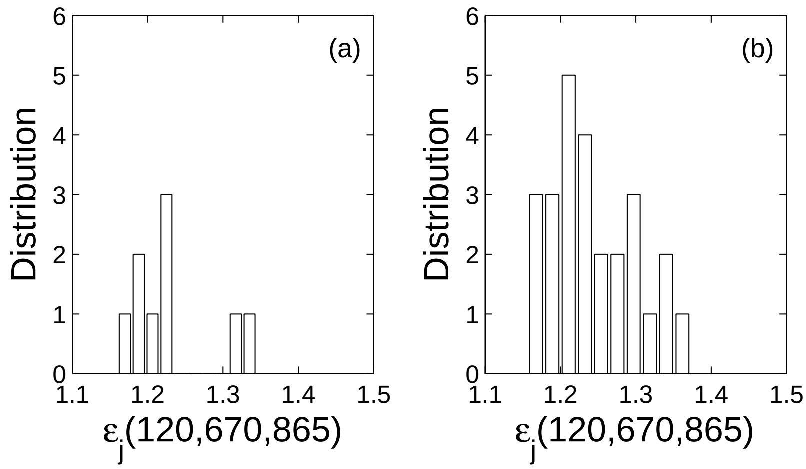

Figure 5.8: Histogram of e(c = 120, 670, 865) for the weakly absorbing neurons (a) and the absorbing neurons (b).

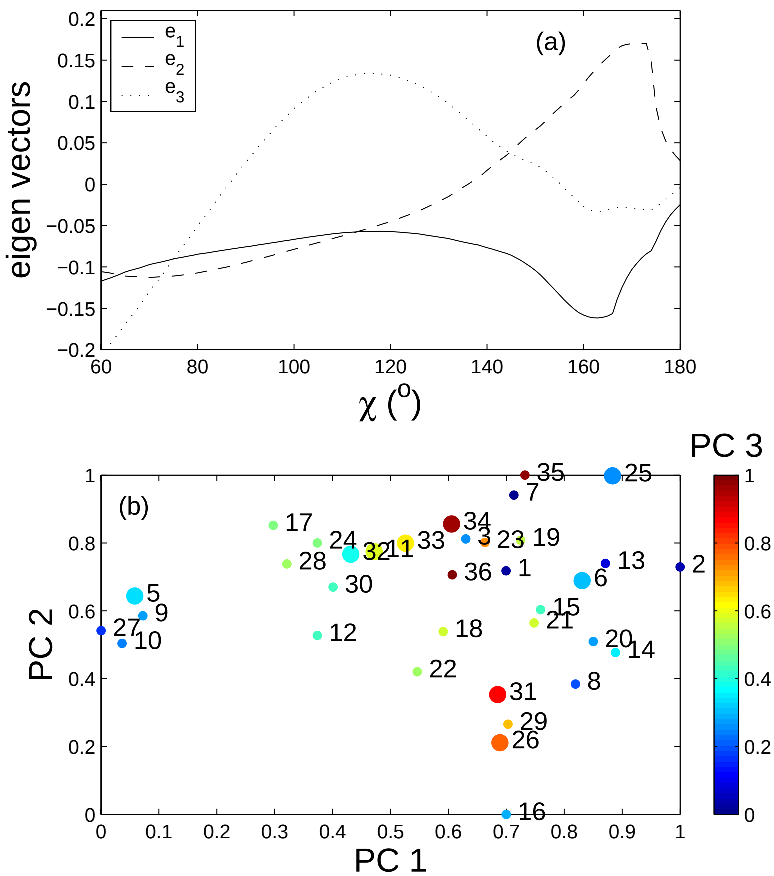

Figure 5.9: The results of a principal component analysis performed on the PRSOM neurons. (a) The first, second, anf third eigen vectors of the $\varepsilon(\chi, 670, 865)$ covariance matrix, for c ranging from 60 to 180^{o}. (b) Three-dimensional plot of the first three principal components (PC) of the PRSOM neurons (encoded between 0 and 1 for commodity). The third PC (PC3) is displayed using a color scale. Small circles denote absorbing neurons and large circles weakly absorbing neurons. The neuron number is indicated in the vicinity of its coordinates.

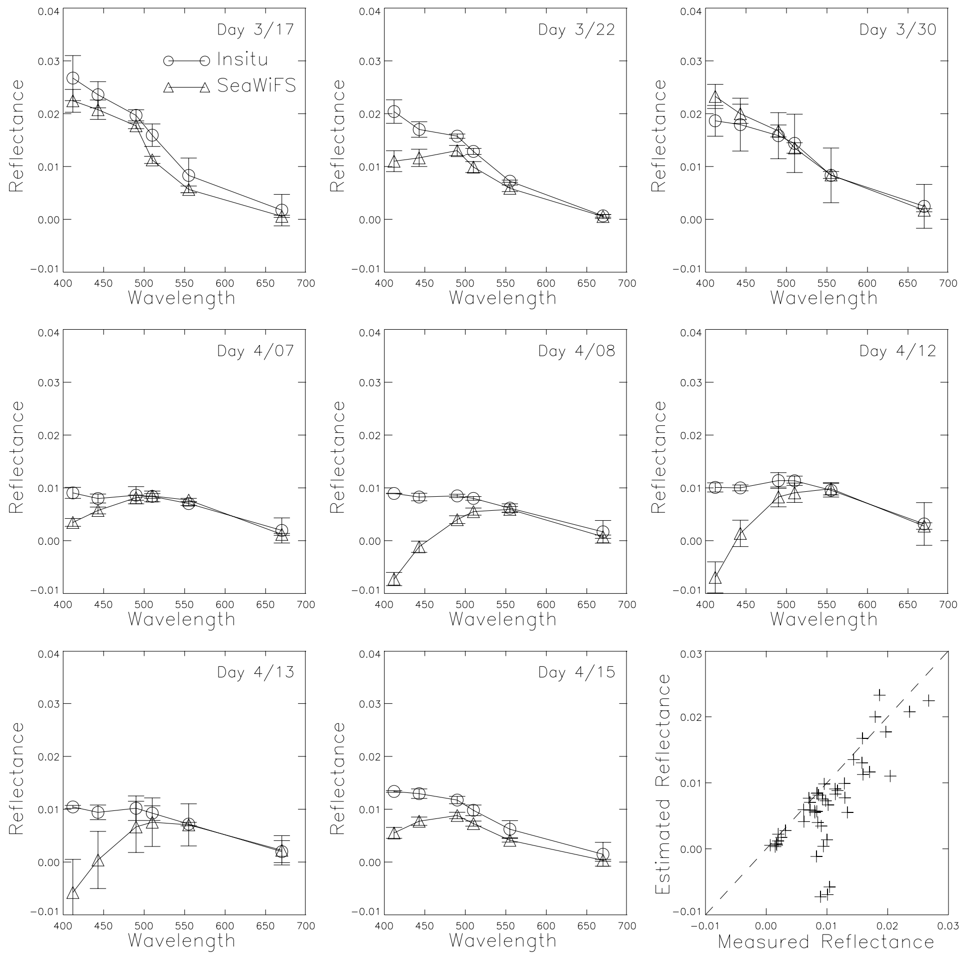

Figure 5.10: SeaWiFS-derived and measured marine reflectance at match-up stations during ACE-Asia. Marine reflectance from SeaWiFS is generally underestimated, especially in the blue.

Thus the two types of mixtures cannot be distinguished. However, within the absorbing mixtures, the dust neurons are easily separated from the urban/soot neurons. In an operational situation, the sampling of the χ space may vary from a pixel to another, but a scalar product between the measured ε and the eigen vectors (displayed in Figure 5.9a) can still be computed, even over a restricted χ range. A simple study made for a POLDER orbit shows that the PRSOM weakly absorbing mixtures can be always separated by computation of their principal components, which may be used in an ocean color processing line. Details about the study can be found in Gross *et al*., (2003) and Gross-Colzy and Frouin (2003).

Evaluation of SeaWiFS-derived marine reflectance and chlorophyll concentration

Marine reflectance, chlorophyll-a concentration, and particulate back-scattering coefficient derived from SeaWiFS imagery have been evaluated in various oceanic regions and atmospheric environments. These include East Asian Seas (Li *et al.*, 2003), the Black Sea and the Eastern Mediterranean Sea (Sancak *et al.*, 2003), and various bio-provinces of the Atlantic Ocean (Frouin *et al.*, 2003).

Figures 5.10 and 5.11 display retrieved and measured marine reflectance and aerosol optical thickness, respectively, at match-up stations during ACE-Asia (R/V Brown cruise). The SeaWiFS marine reflectance is generally lower than the measurements, especially in the blue. The SeaWiFS aerosol optical thickness at 865 nm is larger than the measurements, but its spectral dependence is smaller. Despite the discrepancies, retrieved and measured chlorophyll-a concentrations are in fairly good agreement, with a correlation coefficient squared of 0.78 and a rms difference of 62%. The lower marine reflectance in the blue may be attributed to absorbing aerosols, not only dust, but also sub-micron particles (soot from diesel fuel and coal consumption), as suggested by Li *et al.* (2003).

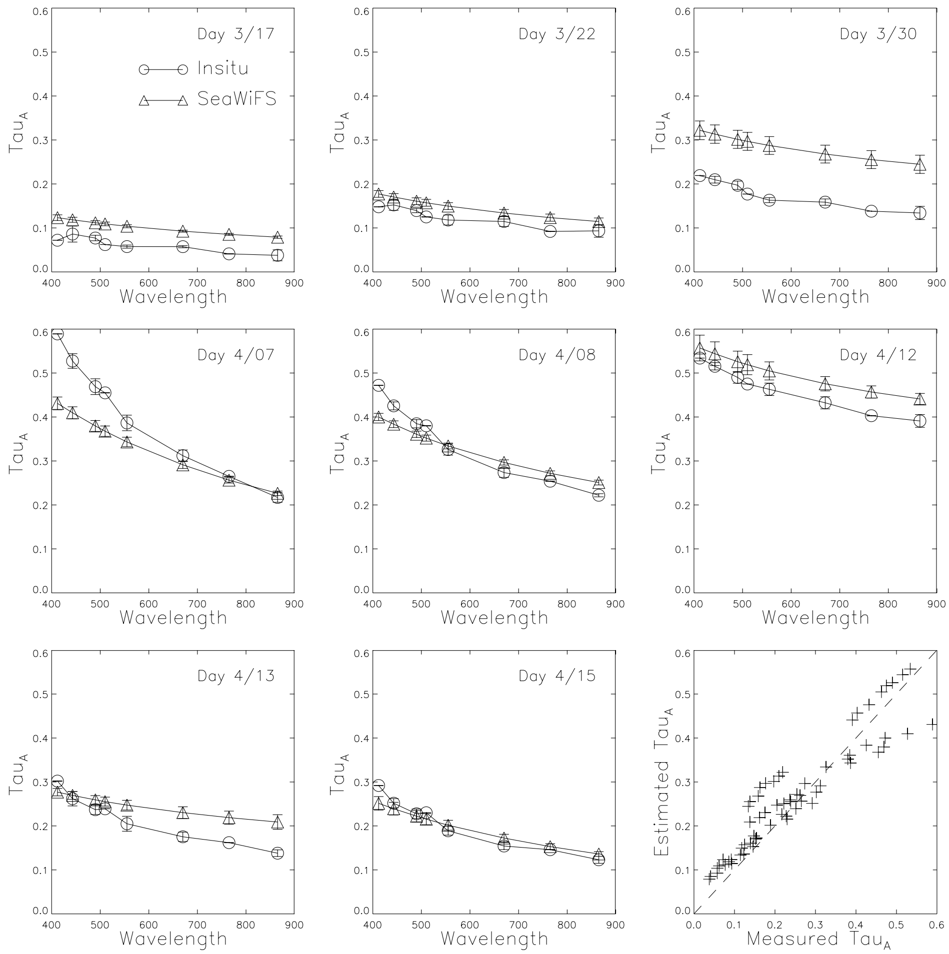

Figure 5.11: SeaWiFS-derived and measured aerosol optical thickness at match-up stations during ACE-Asia. Optical thickness from SeaWiFS is often larger at 865 nm, but its spectral dependence is smaller.

Along Atlantic transects in October-November 2001 and March-April 2002 (R/V Ioffe cruise), SeaWiFS and HPLC chlorophyll-a concentrations agree qualitatively, but there is overestimation by the SeaWiFS algorithm in the oligotrophic waters of both transects (Frouin *et al.*, 2003). Changes in the absolute values and in the form of the spectral absorption of the particulate matter are observed in the waters of different productivity sampled (Fig. 5.12), and such features are important in the development of regional bio-optical algorithms. A general resemblance is noted between particulate back-scattering and chlorophyll distributions. This is not surprising, because back-scattering coefficient depends on particulate matter in seawater that can originate from phytoplankton as a primary source. But the particulate back-scattering distributions (Fig. 5.13) also bear a similarity to the aerosol optical thickness distributions in the central Atlantic (Fig. 5.14), where high values due to transport of Saharan dust occur.

The performance of the OC2 and OC4 algorithms to estimate chlorophyll-a concentrations has also been tested in two contrasted bio-optical environments, the Black Sea and the Mediterranean Sea (Sancak *et al.*, 2003). The in situ bio-optical measurements were made during October 1999 at 25 stations (R/V Bilim cruise). Comparisons of the in situ measurements with the concurrent SeaWiFS retrievals indicate that the OC2 and OC4 algorithms are not working satisfactorily in both seas. Case 2 waters dominate the Black Sea and the failure of the algorithms is expected. On the other hand, failure of the algorithms in the Case 1 waters of the Mediterranean Sea may be due to their specific optical properties. Modifying the OC4 algorithm to include SeaWiFS information at 412 nm yields a better performance in the Mediterranean Sea without degrading performance in the Black Sea. Combining a local algorithm adapted to oligotrophic waters of the Mediterranean Sea and OC4 provides the best results overall.

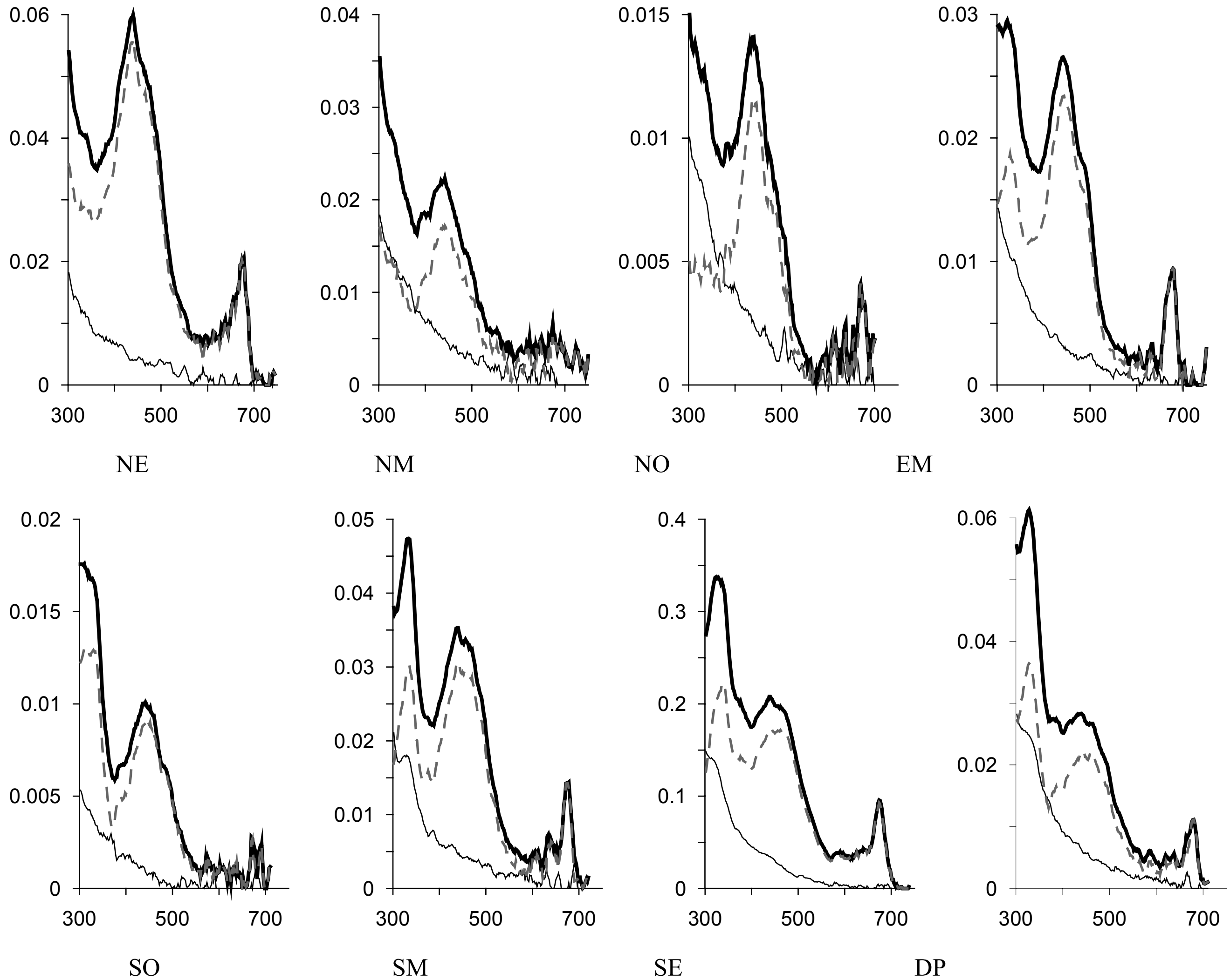

Figure 5.12: Spectra of the absorption coefficients of the particulate matter (thick line), phytoplankton pigment (dash), and detritus (thin line) in different waters in October-November 2001: NE - North eutrophic (Chl=0.77 mg·m^{-3}); NM- North mesotrophic (Chl=0.17 mg·m^{-3}); NO - North oligotrophic (Chl=0.11 mg·m^{-3}); EM - Equatorial mesotrophic (Chl=0.32 mg·m^{-3}); SO - South oligotrophic (Chl=0.07 mg·m^{-3}); SM - South mesotrophic (Chl=0.38 mg·m^{-3}); SE - South eutrophic (Chl=4.9 mg·m^{-3}); DP - Drake Passage (Chl=0.40 mg·m^{-3}).

Atmospheric correction of ocean color via principal component analysis

A methodology has been proposed to retrieve marine reflectance and chlorophyll-a concentration from space by decomposing the satellite reflectance, Rp, into principal components (Gross-Colzy and Frouin, 2003). The components sensitive to the ocean signal (Table 5.2, Fig. 5.15) are combined to retrieve the principal components of marine reflectance, Rw, allowing reconstruction of marine reflectance and estimation of chlorophyll-a concentration. Multi-layered perceptrons are used to approximate the functions relating the useful principal components of satellite reflectance to the principal components of marine reflectance (Fig. 5.16). The algorithm is developed and evaluated using non-noisy and noisy synthetic data sets created for a wide range of angular and geophysical conditions. In the absence of noise on satellite

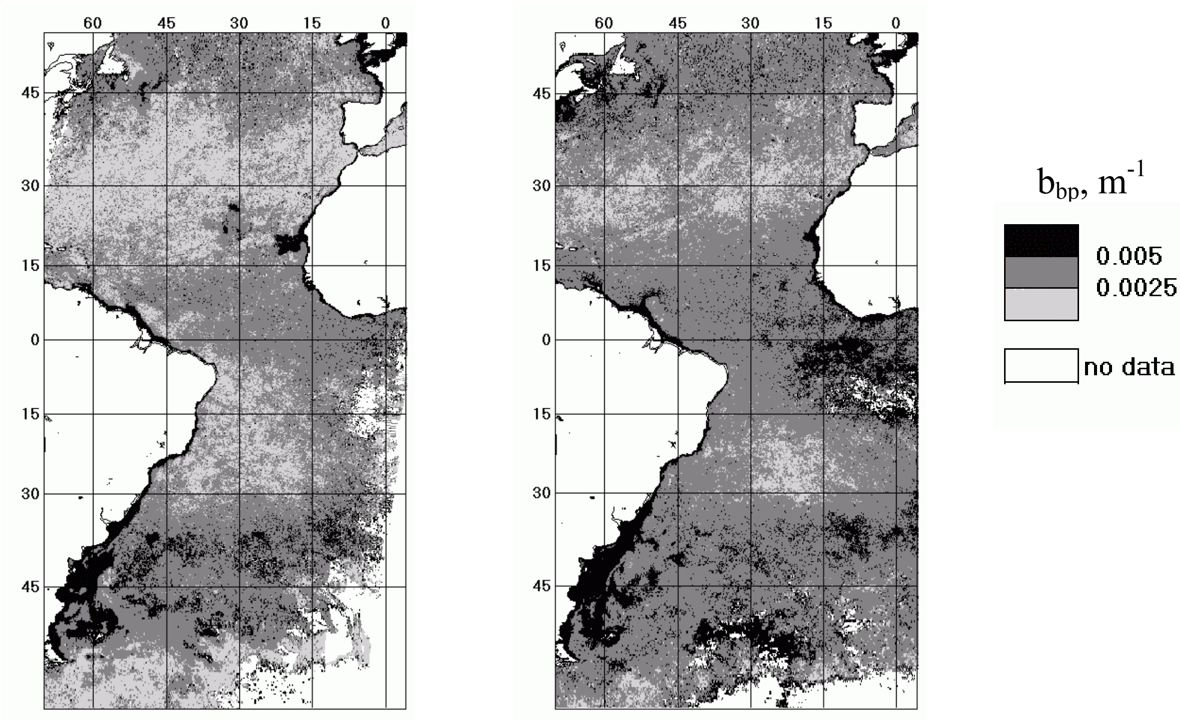

October 2001 October 2002

Figure 5.13: The mean monthly distributions of values of the particle backscattering coefficient in the Atlantic Ocean in October 2001 and 2002 derived from SeaWiFS data.

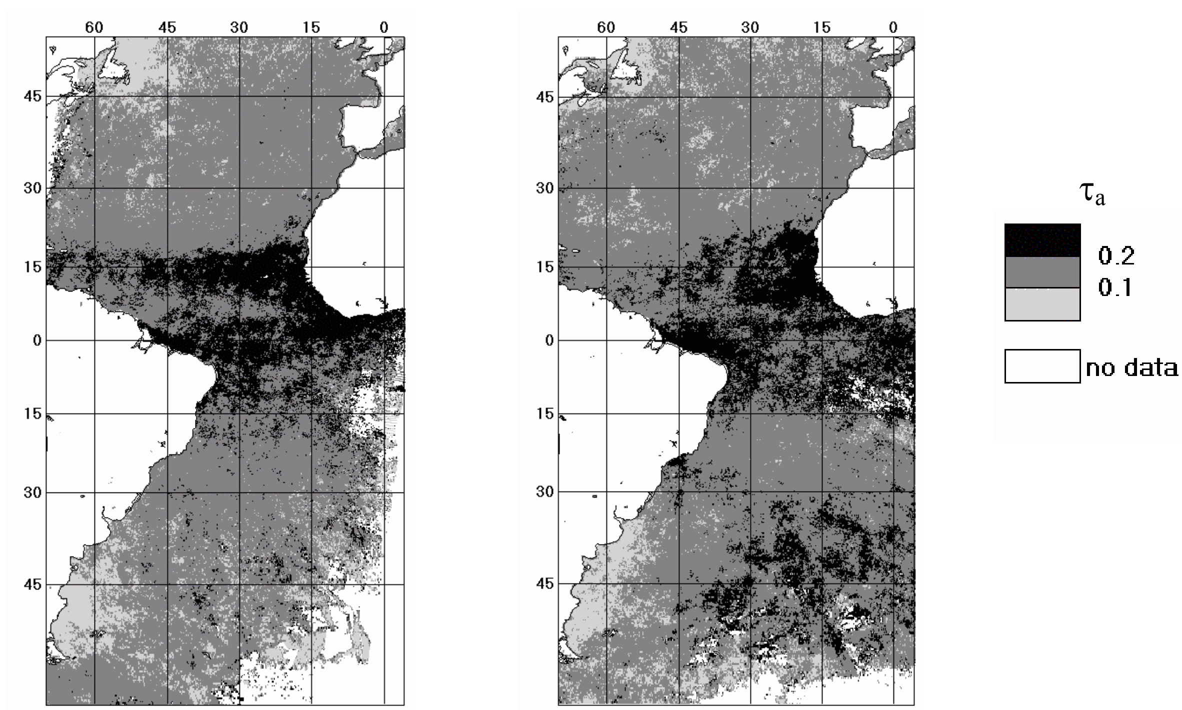

October 2001 October 2002

Figure 5.14: The mean monthly distributions of values of the aerosol optical thickness over the Atlantic Ocean in October 2001 and 2002 derived from SeaWiFS data.

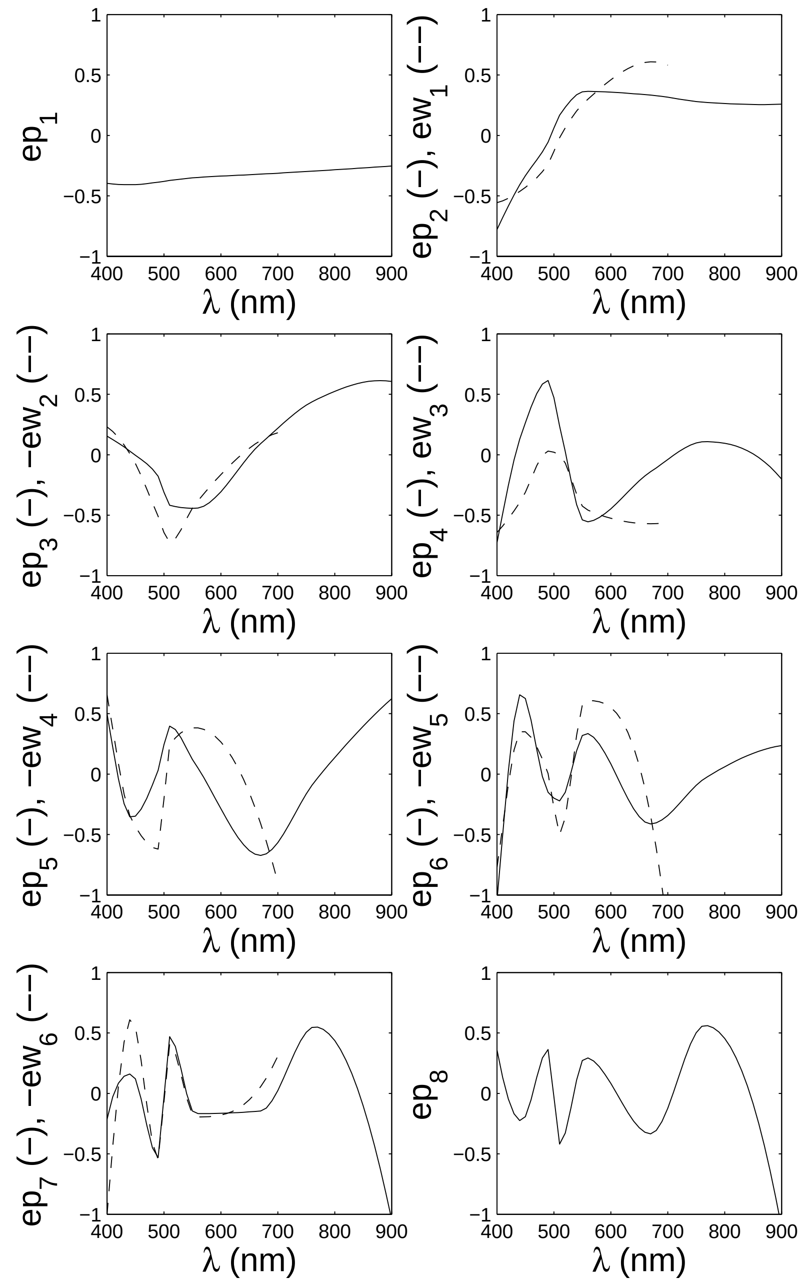

Figure 5.15: Eigenvectors of the *Rp* and *Rw* covariance matrices. The ep_i are displayed for λ ranging from 400 to 900 nm and the ew_j for λ ranging from 400 to 700 nm.

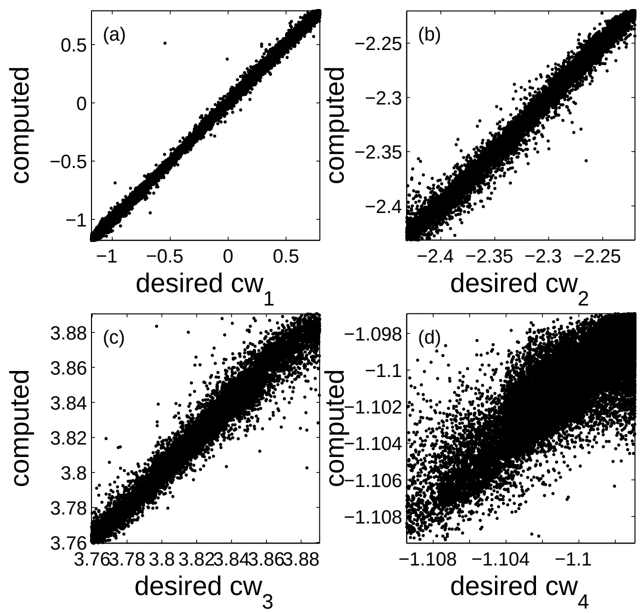

Figure 5.16. Computed versus desired principal components of marine reflectance, cw_j, for $j = 1,\ldots,4$.

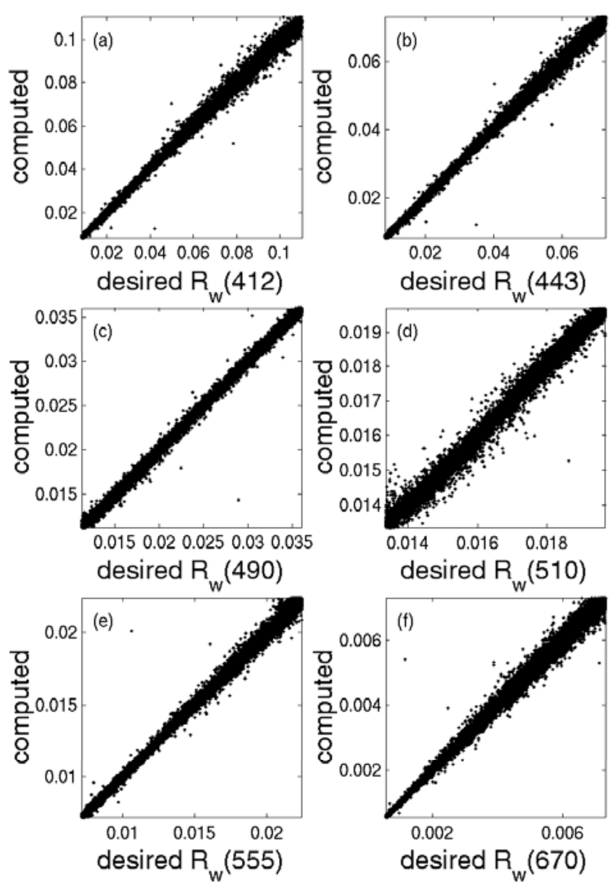

Figure 5.17: Computed versus desired marine reflectance, *Rw*, for 6 SeaWiFS wavelengths: (a) 412, (b) 443, (c) 490, (d) 510), (e) 555, and (f) 670 nm.

reflectance, the relative error on marine reflectance does not exceed 2% (Table 5.3, Fig. 5.17). Accurate retrieval of the first principal component of marine reflectance allows a global relative error of 5.4% on chlorophyll-a concentration (Table 5.3, Figs. 5.18 and 5.19). In the presence of 1% non-correlated and 5% spectrally correlated noise on satellite reflectance, the relative error is increased to 6% and 21%, respectively. Application to SeaWiFS imagery yields marine reflectance and chlorophyll-a concentration fields that resemble those obtained from the standard SeaWiFS processing (Figs. 5.20, 5.21, 5.22 & 5.23), but are generally less contrasted. The marine reflectance spectra retrieved by the two algorithms are substantially different (Fig. 5.22). A large number of SeaWiFS spectra are characterized in the blue by low values not expected in Case-I waters. Accuracy can be improved by including bio-optical variability in the simulated marine reflectance ensembles.

5.4. ACKNOWLEDGMENTS

We wish to thank the officers, technicians, and scientists that have voluntarily collected SIMBAD data and contributed to data analysis, namely Guislain Becu, Jushiro Cepeda-Morales, Martin de La Cruz, Jean-Marc Nicolas, and Haili Wang. We also gratefully John McPherson for programming support, and the SeaWiFS and SIMBIOS project staff for helping with match-up data and for stimulating discussions. This work is supported by the National Aeronautics and Space Administration under contract NAS5-00194, the Scripps Institution of Oceanography, the California Space Institute, the Centre National d'Etudes Spatiales, and the Centre National de la Recherche Scientifique.

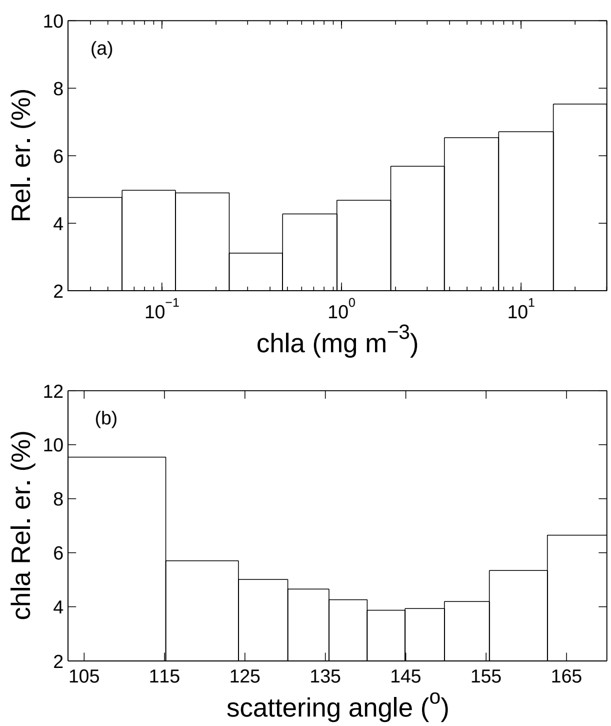

Figure 5.18: Relative error (%) on chlorophyll concentration, *chla*, as a function of (a) *chla* and (b) scattering angle.

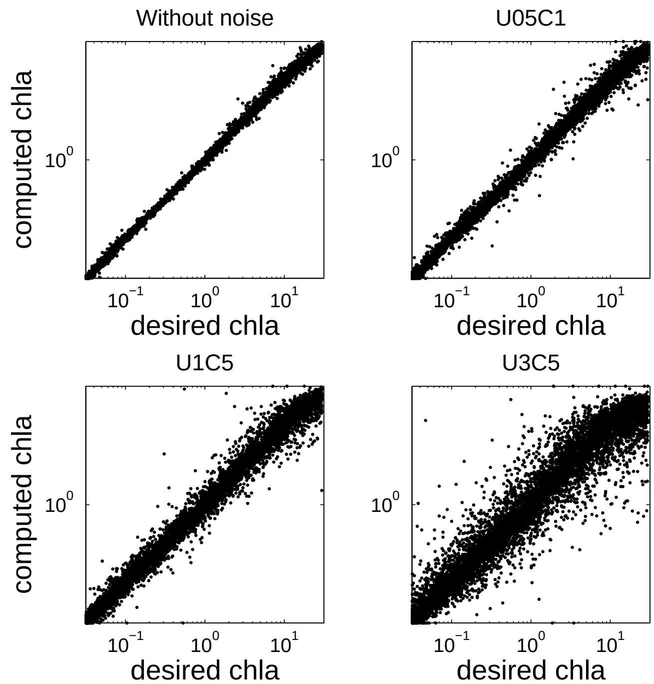

Figure 5.19: Computed versus desired chlorophyll concentration, chl *a*, for various noise figures (see text for details).

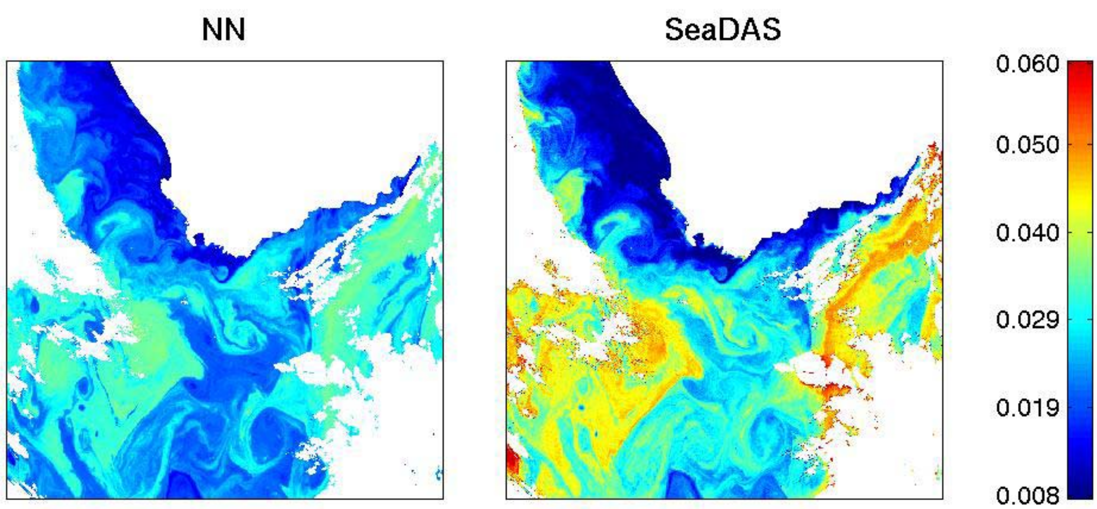

Figure 5.20: Marine reflectance at 443 nm, *Rw(443)*, derived using neural network (left) and SeaDAS (right), for SeaWiFS imagery acquired off South Africa on February 14, 1999.

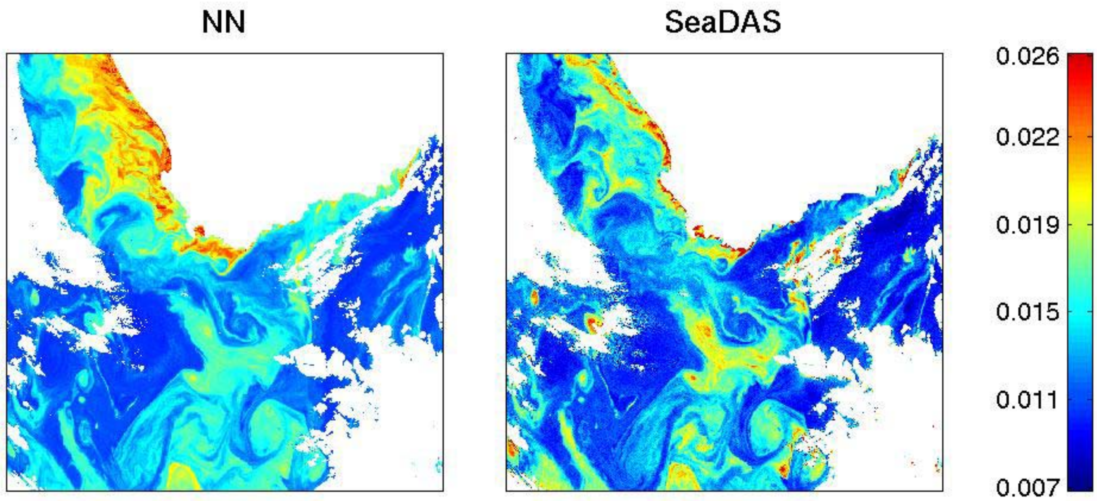

Figure 5.21: Marine reflectance at 555 nm, *Rw(555)*, derived using neural network (left) and SeaDAS (right), for SeaWiFS imagery acquired off South Africa on February 14, 1999.

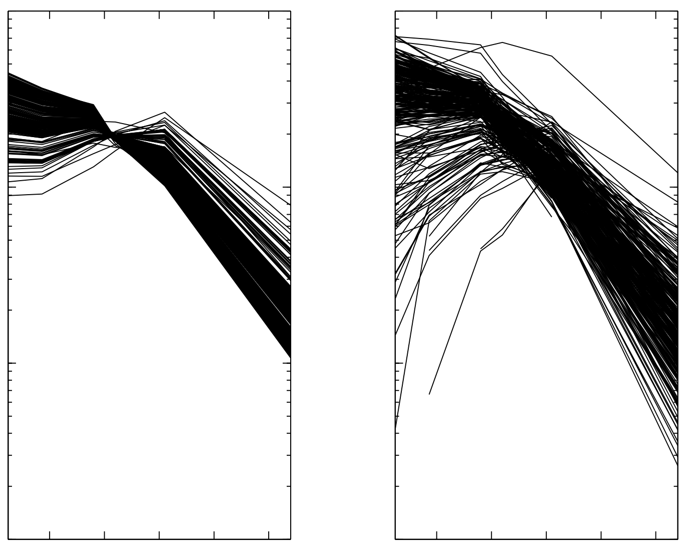

Figure 5.22: Selected marine reflectance spectra, *Rw(λ)*, obtained using neural network (left) and SeaDAS (right), for SeaWiFS imagery acquired off South Africa on February 14, 1999.

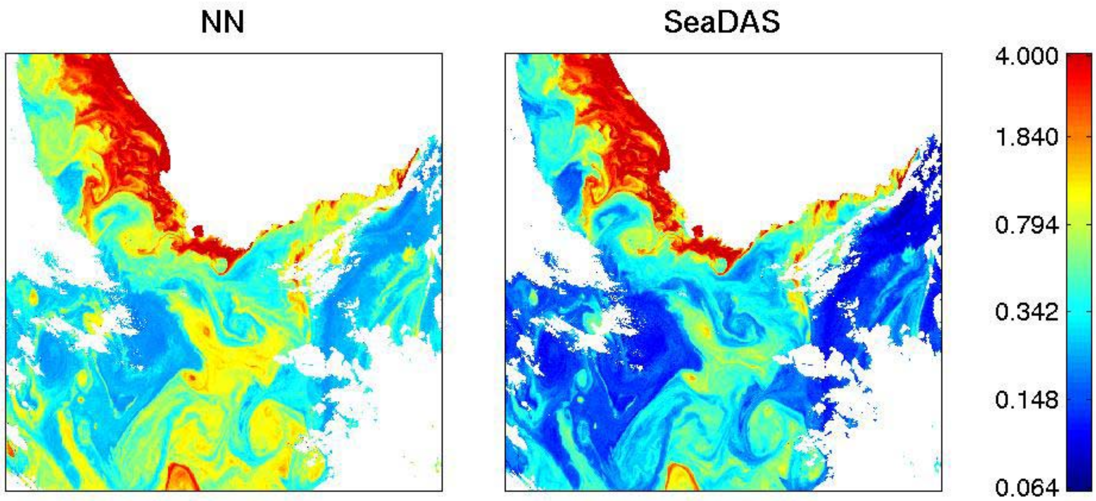

Figure 5.23. Chlorophyll concentration, chl*a*, in mgm^{-3} derived from neural network (left) and SeaDAS (right), for SeaWiFS imagery acquired off South Africa on February 14, 1999.

Table 5.2: Correlation coefficients (%) between the eight principal components of ***Rp***, cp_i, and the six principal components of ***Rw***, cw_j. The correlation coefficients between the cp_i and $\tau(550)$ and chl*a* are also indicated.

	cp_1	cp_2	cp_3	cp_4	cp_5	cp_6	cp_7	cp_8
cw_1	12.3	73.3	-39.8	-47.4	16.9	-0.1	-5.7	-8.9
cw_2	2.8	17.6	-17.4	56.0	63.6	1.8	29.8	21.2
cw_3	3.9	12.0	-2.3	46.8	10.3	-22.9	-45.2	-40.5
cw_4	1.2	3.7	-1.6	9.9	-5.3	44.1	-58.1	26.5
cw_5	0.0	-1.0	1.2	-3.1	2.0	-38.6	14.7	-14.5
cw_6	-0.2	0.1	0.2	-1.3	0.3	-12.9	-4.4	12.0
$\tau(550)$	-67.6	22.4	-4.2	15.8	-22.6	22.3	19.9	-38.2
chla	12.1	71.6	-38.0	-51.4	11.0	-0.3	-10.0	-11.3

Table 5.3: Mean performance of the neural network algorithm in the absence of noise. The tests are performed on the whole data ensemble, the RMS error and bias are computed in the physical units of each parameter (in mgm^{-3} for chl*a*).

	RMS Err.	Rel. Err. (%)	R^2 (%)	Bias
Rw(412)	0.0012	1.7	99.9	0.0000
Rw(443)	0.0007	1.4	99.9	0.0000
Rw(490)	0.0003	0.8	99.9	0.0000
Rw(510)	0.0001	0.5	99.7	0.0000
Rw(555)	0.0002	0.9	99.9	0.0000
Rw(670)	0.0001	1.8	99.9	0.0000
chla	0.841	5.4	99.3	0.0467

REFERENCES

Li, L. P., H. Fukushima, R. Frouin, B. G. Mitchell, M. X. He, T. Takamura, and S. Ohta, 2003: Influence of absorbing aerosols on SeaWiFS-derived marine reflectance during ACE-Asia. In *Ocean Remote Sensing and Applications*, R. Frouin, Y. Yuan, and H. Kawamura, Editors, Proceedings of SPIE Vol. **4892**, pp. 105-115.

Li, L. H. Fukushima, R. Frouin, B. G. Mitchell, M-X He, I. Uno, T. Takamura, and S. Ohta, 2003: Influence of sub-micron absorptive aerosol on SeaWiFS-derived marine reflectance during ACE-Asia, *J. Geophys. Res*.,in press.

Frouin, R., O. Kopelevich, V. Burenkov, A. Demidov, A. Grigoriev, A. Khrapko, S. Sheberstov, and S. Vazyulya, 2003: Variability of the bio-optical characteristics on the Atlantic transect between 50^{o}N and 55^{o}S in two different seasons from satellite and ship data. In *Current Problems in Optics of natural Waters*, K. Shifrin, I. Levin and G. Gilbert, Editors, Proceedings of ONW-2003, Saint-Petersburg, Russia, in press.

Gross-Colzy, L., R. Frouin, C. M. Pietras, and G. S. Fargion, 2003: Non-supervised classification of aerosol mixtures for ocean color remote sensing. *Ocean Remote Sensing and Applications*, R. Frouin, Y. Yuan, and H. Kawamura, Editors, Proceedings of SPIE Vol. **4892**, pp. 95-104.

Gross-Colzy, L., and R. Frouin, 2003: Self-organized mapping of aerosol mixtures at AERONET coastal and island sites. *IEEE Neural Network for Signal Processing Workshop 2003*, Toulouse, France, in press.

Sancak, S., S. T. Besiktepe, a. Yilmaz, M. Lee, B. G. Mitchell, and R. Frouin, 2003: Evaluation of SeaWiFS chlorophyll-a in the Black and Mediterranean Seas. *Int. J. Remote Sensing*, accepted.

Shettle E.P. and R.W. & Fenn, 1979: Models for the aerosol of the lower atmosphere and the effects of humidity variations on their optical properties. AFGL Tech. Rep., **105**, D8, 9-887-9901.

This Research was Supported by the NASA Contract # 00194

Publications

Deschamps, P.-Y., B. Fougnie, R. Frouin, P. Lecomte, and C. Verwaerde, 2003: SIMBAD: A field radiometer for satellite ocean-color validation. *Appl. Opt*., submitted.

Dubuisson, P., D. Dessailly, M. Vesperini, and R. Frouin, 2003: Water vapor retrieval over ocean using near-infrared radiometry. *J. Geophys. Res*., submitted.

Frouin, R., and S. F. Iacobellis, 2002: Influence of phytoplankton on the global radiation budget. *J. Geophys. Res*., **107**, 4377, doi: 10.1029/2001JD000562.

Frouin, R., and G. D. Gilbert, Editors, 2002: *Remote Sensing and Underwater Imaging*. Proceedings of SPIE Vol. **4488**, 280 pp. Published by SPIE--The International Society for Optical Engineering, Bellingham, Washington, USA. [Book]

Frouin, R., G. D. Gilbert, and D. Pan, Editors, 2003*: Ocean Remote Sensing and Imaging II*. Proceedings of SPIE Vol. **5155**, in press. Published by SPIE –the International Society for Optical Engineering, Bellingham, Washington, USA.[Book]

Frouin, R., Y. Yuan, and H. Kawamura, Editors, 2003: *Ocean Remote Sensing and Applications*. Proceedings of SPIE Vol. **4892**, 620 pp. Published by SPIE--The International Society for Optical Engineering, Bellingham, Washington, USA. [Book]

Frouin, R., L. Gross-Colzy, and P.-Y. Deschamps, 2003: Ocean color remote sensing without explicit atmospheric correction. In *Ocean Remote Sensing and Applications*, R. Frouin, Y. Yuan, and H. Kawamura, Editors, Proceedings of SPIE Vol. **4892**, pp. 133-142.

Frouin, R., B. A. Franz, and P. J. Werdell, 2003: The SeaWiFS PAR product. In *Algorithm Updates for the Fourth SeaWiFS Data Reprocessing*, S. B. Hooker and E. R. Firestone, Editors, NASA/TM-2003-206892, Vol. **22**, pp. 46-50.

Frouin, R., O. Kopelevich, V. Burenkov, A. Demidov, A. Grigoriev, A. Khrapko, S. Sheberstov, and S. Vazyulya, 2003: Variability of the bio-optical characteristics on the Atlantic transect between 50^oN and 55^oS in two different seasons from satellite and ship data. In *Current Problems in Optics of natural Waters*, K. Shifrin, I. Levin and G. Gilbert, Editors, Proceedings of ONW-2003, Saint-Petersburg, Russia, in press.

Fukushima, H., M. Toratani, A. Tanaka, W. Chen, H. Murakami, R. Frouin, and B. G. Mitchell, 2003: ADEOS-II/GLI ocean color atmospheric correction: Early phase result. In *Ocean Remote Sensing and Imaging II*, R. Frouin, G. D. Gilbert, and D. Pan, Editors, Proceedings of SPIE Vol. **5155**, in press.

Gross-Colzy, L., and R. Frouin, 2003a: Self-organized mapping of aerosol mixtures at AERONET coastal and island sites. *IEEE Neural Network for Signal Processing Workshop 2003*, Toulouse, France, in press.

Gross-Colzy, L., R. Frouin, C. M. Pietras, and G. S. Fargion, 2003: Non-supervised classification of aerosol mixtures for ocean color remote sensing. In *Ocean Remote Sensing and Applications*, R. Frouin, Y. Yuan, and H. Kawamura, Editors, Proceedings of SPIE Vol. **4892**, pp. 95-104.

Gross-Colzy, L., and R. Frouin, 2003b: Remote sensing of chlorophyll concentration from space by principal component analysis of atmospheric effects. In *Ocean Remote Sensing and Imaging II*, R. Frouin, G. D. Gilbert, and D. Pan, Editors, Proceedings of SPIE Vol. **5155**, in press.

Gross-Colzy, L., C. Dupouy, R. Frouin, J.-M. André, and S. Thiria, 2003: Reducing variability due to secondary pigments in the retrieval of chlorophyll concentration from marine reflectance: A case study in the western equatorial Pacific. *Appl. Opt*., submitted.

Knapp, K., R., and R. Frouin, 2003: Separating the aerosol signal from surface effects in geostationary satellite measurements. *J. Geophys. Res*., submitted.

Li, L. H. Fukushima, R. Frouin, B. G. Mitchell, M-X He, I. Uno, T. Takamura, and S. Ohta, 2003: Influence of sub-micron absorptive aerosol on SeaWiFS-derived marine reflectance during ACE-Asia, *J. Geophys. Res*., in press.

Li, L. P., H. Fukushima, R. Frouin, B. G. Mitchell, M. X. He, T. Takamura, and S. Ohta, 2003: Influence of absorbing aerosols on SeaWiFS-derived marine reflectance during ACE-Asia. In *Ocean Remote Sensing and Applications*, R. Frouin, Y. Yuan, and H. Kawamura, Editors, Proceedings of SPIE Vol. **4892**, pp. 105-115.

Loisel, H., J.-M. Nicolas, P.-Y. Deschamps, and R. Frouin, 2002: Seasonal and inter-annual variability of particulate organic matter in the global ocean. *Geophys. Res. Lett*., **29**, doi:10.1029/2002/GL015948.

Meister, G., P. Abel, R. Barnes, J. Cooper, C. Davis, G. Fargion, R. Frouin, M. Godin, D. Korwan, R. Maffione, C. McClain, S. McLean, D. Menzies, A. Poteau, J. Robertson, and J. Sherman, 2003: Comparison of spectral radiance calibrations at oceanographic and atmospheric research laboratories. *Metrologia*, **40**, pp. S93-S96.

Miller, A. J., M. A. Alexander, G. J. Boer, F. Chai, K. Denman, D. J. Erikson, R. Frouin, A. Gabric, E. Laws, M. Lewis, Z. Liu, R. Murtugudde, S. Nakamoto, D. J. Nielson, J. R. Morris, C. Ohlman, I. Perry, N. Schneider, K. Shell, and A. Timmermann, 2003: Potential feedbacks between Pacific Ocean ecosystems and inter-decadal climate variations. *Bull. Am. Meteor. Soc*., **84**, pp. 617-633.

Nakamoto, S. S. Prasanna-Kumar, J. M. Oberhuber, H. Saito, K. Muneyama, and R. Frouin, 2002: Chlorophyll modulation of mixed layer thermodynamics in a mixed layer-sopycnal general circulation model--An example from the Arabian Sea and the Equatorial Pacific. *Proc. Indian Acad. Sci. (Earth Planet. Sci.)*, **111**, pp. 339-349.

Nakamoto, S., K. Muneyama, T. Sato, S. Prasanna Kumar, A. Kumar, and R. Frouin, 2002: Ocean bio-geophysical modeling using mixed layer-isopycnal general circulation model coupled with photosynthesis process. *Recent Research Development in Geophysics*, **4**, pp. 9-20, Researchsigpost, Trivandrum-695 023, Kerala, India.

Nakamoto, S. S. Prasanna-Kumar, K. Nakata, K. Shell, R. Frouin, K. Ueyoshi, P. Sammarco, A. Lai, H. Saito, T. Sato, and K. Muneyama, 2003: Thermophysical Interaction of Ocean Ecosystem and Geophysical system--For Understanding Carbon Circulation in the Ocean. *J. Adv. Mar. Sci. Tech. Soc*., **8**, pp. 35-48.

Sancak, S., S. T. Besiktepe, a. Yilmaz, M. Lee, B. G. Mitchell, and R. Frouin, 2003: Evaluation of SeaWiFS chlorophyll-a in the Black and Mediterranean Seas. *Int. J. Remote Sensing*, accepted.

Shell, K., R. Frouin, S. Nakamoto, and R. C. J. Somerville, 2003: Atmospheric response to solar radiation absorbed by phytoplankton, *J. Geophys. Res*., **108**, doi: 10.1029/2003JD003440.

Smirnov, A., B. N. Holben, O. Dubovik, R. Frouin, and I. Slutsker, 2003: Maritime component in aerosol optical models derived from AERONET (Aerosol Robotic Network) data, *J. Geophys. Res*., **108**, 4033, doi: 10.1029/2002JD002701.

Souaidia, N., C. Pietras, S. Brown, K. Lykke, P.-Y. Deschamps, G. Fargion, and B. C. Johnson, 2003: Sun photometer laser- and lamp-based radiometric calibrations: Comparison with the Langley technique and implications on remote sensing. In *Ocean Remote Sensing and Imaging II*, R. Frouin, G. D. Gilbert, and D. Pan, Editors, Proceedings of SPIE Vol. **5155**, in press.

Zhao, X.-P., I. Laszlo, O. Dubovik, A. Smirnov, B. H. Holben, J. Sapper, C. Pietras, K. J. Voss, and R. Frouin, 2003: Regional evaluation of the revised NOAA/NESDIS AVHRR two-channel aerosol retrieval algorithm and determination of the refractive index for key aerosol types over the ocean. *J. Geophys. Res*., in press.